Data-Driven Approaches for Measurement Interpretation: Analysing Integrated Thermal and Vehicular Response in Bridge Structural Health Monitoring

Rolands Kromanis[*,a] and Prakash Kripakaran*[b]

[a] *Civil Engineering Department, Nottingham Trent University, UK;* [b] *College of Engineering, Mathematics and Physical Sciences, University of Exeter, UK.*

Abstract: A comprehensive evaluation of a structure's performance based on quasi-static measurements requires consideration of the response due to all applied loads. For the majority of short- and medium-span bridges, temperature and vehicular loads are the main drivers of structural deformations. This paper therefore evaluates the following two hypotheses: (i) knowledge of loads and their positions, and temperature distributions can be used to accurately predict structural response, and (ii) the difference between predicted and measured response at various sensor locations can form the basis of anomaly detection techniques. It introduces a measurement interpretation approach that merges the regression-based thermal response prediction methodology that was proposed previously by the authors with a novel methodology for predicting traffic-induced response. The approach first removes both environmentally (temperature) and operationally (traffic) induced trends from measurement time series of structural response. The resulting time series is then analysed using anomaly detection techniques. Experimental data collected from a laboratory truss is used for the evaluation of this approach. Results show that (i) traffic-induced response is recognized once thermal effects are removed, and (ii) information of the location and weight of a vehicle can be used to generate regression models that predict traffic-induced response. As a whole, the approach is shown to be capable of detecting damage by analysing measurements that include both vehicular and thermal response.

Keywords: structural health monitoring, long-term bridge monitoring, thermal response, temperature effects, signal processing, anomaly detection

Abbreviations

TIC – thermal imaging camera;
RBTRP – regression-based thermal response prediction;
TIRP – traffic-induced response prediction;
PE – prediction error;
PCA – principal component analysis;
SVR – support vector regression;
SSM – signal subtraction method.

1. Introduction

Bridges are important transportation links, and their uninterrupted operation is vital for a functioning economy and society. Current procedures for their structural management are based largely on visual inspections that can be unreliable and highly subjective [1,2]. Furthermore, since detailed visual inspections are expensive requiring significant engineer time, they are performed sporadically. For example, in the UK, principal inspections that require engineers to examine each bridge component by getting within touching distance are

typically performed only once every 6 years [3]. Consequently, concerns affecting bridge performance are often identified at an advanced stage, thereby requiring expensive structural interventions that are disruptive to the operation of transport networks. Such reactive approaches to bridge management also leads to huge maintenance backlogs that greatly undermines the capacity of the transport infrastructure. In the UK, the maintenance backlog for works on the 57,000 bridges, which are owned and operated by the local highway authorities and estimated to be worth £24 billion, was over £2.4 billion or about 10% of their value as per 2007 estimates [4]. In the USA, according to data submitted to Federal Highways Administration in 2015, 58,791 bridges (9.6% of the bridge stock) were classified as structurally deficient [5] and the total costs of their rehabilitation were predicted to be $31 billion. There is therefore great interest among the bridge engineering community in deploying sensing technologies, which can provide reliable, continuous data streams about bridge loading and response, as a useful complement to visual inspections [6–9].

The main challenge in sensing-based bridge management is in relating collected measurements to structural performance. Response time histories can be complex to analyse for a variety of reasons. They contain a certain degree of noise due to sensor characteristics. Outliers arising from occasional sensor malfunction or data acquisition issues are also often present. However, more important is the fact that the structural response and hence the measurements are strongly affected by the various loads on the structure including environmental factors and vehicular traffic. Previous research has shown that environmental loads, which vary both diurnally and seasonally, leave a strong signature in the response time histories [10]. Specifically, temperature effects on bridge response can exceed those of other environmental and operational loads [11]. Traffic induced-response appear as short spikes superimposed on thermal response [12]. For example, Figure 1 (left) shows time histories of the horizontal movement measured at the expansion joint of the River Exe Bridge. Spikes in the horizontal movement are induced by heavy vehicles crossing the bridge. Figure 1 (right) is a zoomed-in view of a portion of the displacement time-history that corresponds to the passage of a heavy truck over the bridge. Consequently, simple approaches for detecting damage that ignore how the response is affected by the various loads are not useful for real-life structures. For example, the concept of detecting damage by using threshold bounds on individual measurements seldom works since the effect of damage on structural response is often much smaller than the change in response due to diurnal and seasonal temperature variations [13].

Data-driven techniques that exploit patterns arising from spatial and temporal correlations in measurements are well-suited to deal with the above-mentioned complexities in measured response time histories. Since these techniques do not rely on a physics-based model of the structure, they can be more effective than model-based methods for dealing with the potentially large volumes of measured data. Data-driven techniques usually require a training data-set comprising measurements representing baseline conditions of a bridge. The techniques extract features representative of normal structural behaviour from the training data-set and then compare these features with those extracted from new measurements to detect changes in structural behaviour [14].

Data-driven techniques are adapted typically from quantitative fields such as econometrics [15] and statistics [16]. However, a few techniques such as mathematical correlation models [17] and linear approaches to modelling nonlinearities [18] have also been developed specifically for interpreting bridge monitoring data. The majority of currently available data-driven techniques are concerned with the interpretation of response time histories and are able to detect the onset of damage only in simulated measurements created using numerical models of bridges that model damage as a reduction in stiffness [16]. They fail to demonstrate similar performance for measurements from real-life structures particularly when damage is located away from sensors [19] due to the presence of environmental trends that mask damage effects on response. Laory et al. [20] hence studied the removal of seasonal variations from measurements through use of a moving average filter and a low-pass filter. However, this had the negative effect of reducing damage detectability. Laory et al. [21] later combined two data-driven methods, specifically moving principal component analysis with robust regression analysis, to enhance damage detectability. However, the performance of the resulting approach has been illustrated only on measurements collected during the construction phase of a bridge.

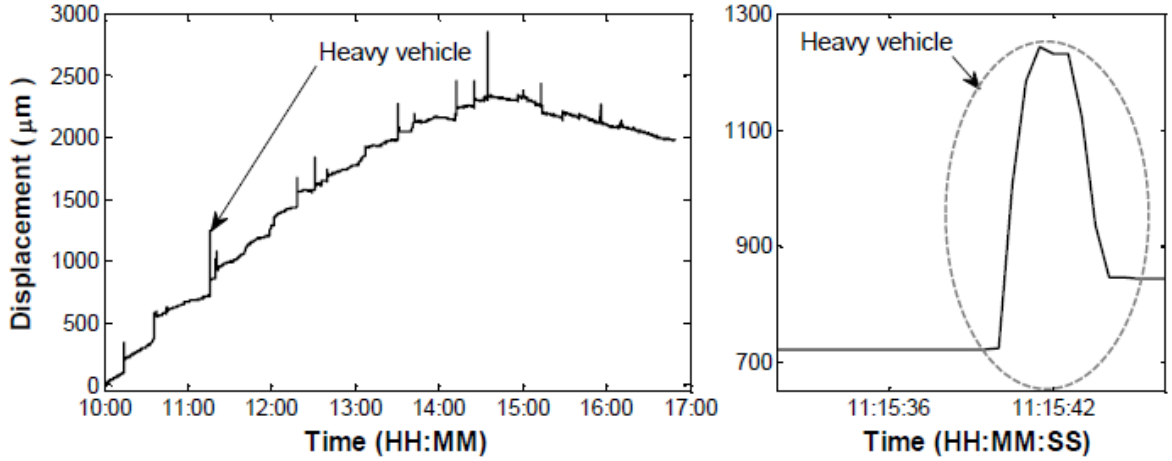

Figure 1 The River Exe Bridge: time histories of the horizontal movement of the steel girder at the expansion joint collected over 7 hours (left) and during the passage of a heavy vehicle (right). (Courtesy: Dr David Hester and Devon County Council.)

Kromanis and Kripakaran [22] suggested a novel data-driven methodology referred to as Regression-Based Thermal Response Prediction (RBTRP) methodology for predicting thermal response, which is the main constituent of the environmental trend in measured response time histories. They demonstrated that measurements of temperature distributions can be exploited to predict accurately thermal effects in measured response. They also showed that the time histories resulting from subtracting the predicted thermal response from the measured response time histories can be analysed by anomaly detection techniques for damage detection. Other researchers have also since investigated similar methods that use both temperature and deformation measurements for damage detection. Yarnold et al [23] showed that distributed temperature and deformation measurements can enable damage detection albeit through the use of physics-based (finite element) models. This research aims to combine the authors' previous work in predicting thermal response with a novel methodology for predicting vehicular response in order to create a damage detection approach that is capable of analysing

response time histories containing both temperature and vehicular effects. There are no data-driven approaches that currently offer this capability.

This study will rely on knowledge of vehicular loads and their positions on the bridge to predict vehicular response. Technologies for measuring vehicle load and location are now well-developed. For example, coupling data from vision-based systems with data from other sensing devices can enable identification of the location, number and types of vehicles, hence, supporting the characterization of their induced response. Such concepts have already been demonstrated in many studies. Glisic et al. [24] have proposed data management principles for accessing and visualizing measurements collected with contact sensors and video streaming. The background subtraction method has been shown to be useful to analyse video-streamed images to identify location, type and speed of a vehicle for anomaly detection [25]. Axle loads of a vehicle can be determined using weigh-in-motion sensors [26]. Video streams of traffic from a bridge have also been combined with displacement measurements to create influence lines, which then serve as input features into anomaly detection methodologies [25]. Therefore, this paper examines how to utilise the knowledge of vehicular and environmental loads, which are increasingly available through measurements from continuous monitoring, to better understand real-time structural performance.

This paper will first describe the overall approach for measurement interpretation including how it will combine methodologies for predicting thermal and vehicular response in a framework for anomaly (damage) detection. This will be followed by a background on the RBTRP methodology for predicting thermal response, and then a description of the novel Traffic-Induced Response Prediction (TIRP) methodology to predict vehicular response. It will later discuss the anomaly detection techniques used to analyse the time histories produced after subtracting thermal and vehicular response from the measured response time histories. The overall approach will be illustrated using measurements collected from a truss that has been built and continuously monitored in the structures laboratory at the University of Exeter. The paper will finish with a discussion of the results, conclusions and limitations of the work.

2. Measurement interpretation approach

The premise of this study is that information of inputs (loads) into and outputs (response) from a structural system are available via monitoring. The vision is to develop separate data-driven methodologies to predict the structural response due to each load and ambient parameter. This will enable filtering the effects of vehicular and environmental loads from measured response time histories and then analysing the resulting time histories using anomaly detection methods. As a first step towards this goal, traffic and temperature effects alone are considered in this research. All other environmental factors (e.g. wind) are assumed to have no effect on a bridge's structural response. The overall measurement interpretation approach is schematically illustrated in Figure 2. Predictions from two methodologies: (1) the RBTRP methodology and (2) TIRP methodology are used to filter thermal and vehicular response respectively from measured response. Both the methodologies for predicting structural response, in order to be useful for real-time measurement interpretation, have to be computationally inexpensive and

potentially applicable to a range of structures. Regression-based models that capture the relationship between structural deformations (e.g. strain, displacement) and loadings (e.g. temperature, traffic) and their locations are well-suited for this task [22], and therefore form the basis of the RBTRP and TIRP methodologies. The time histories resulting from subtracting the predicted thermal and vehicular response from measured response time histories are effectively response-free signals. Response-free signals would be zero signals if the traffic- and temperature-induced response are predicted perfectly by the corresponding methodologies, and if the measurements were free of noise and outliers. These response-free signals are subsequently analysed for anomalies using signal processing techniques. All the elements of the overall approach starting with the RBTRP methodology are described in the following subsections.

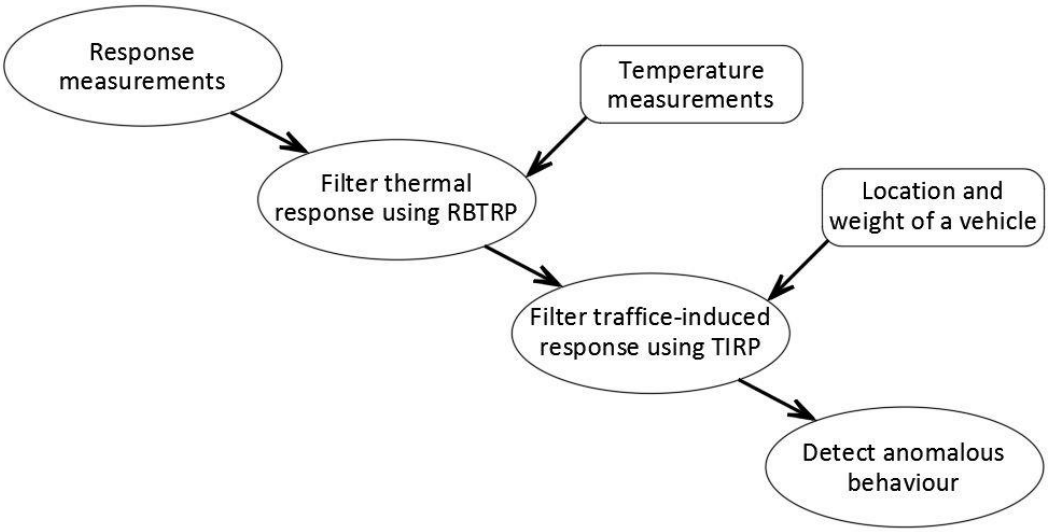

Figure 2 A schematic of the proposed measurement interpretation approach.

2.1. Regression-based thermal response prediction (RBTRP) methodology

The RBTRP methodology is built on a premise that the thermal response of a bridge can be determined from knowledge of its current temperature distributions and an understanding of the relationship between temperature distributions and structural response obtained from a set of reference measurements. The RBTRP methodology consists of the following two phases as shown in Figure 3.

1) Model generation phase: This phase generates regression models that use information of temperature distributions as input to predict thermal response. It involves a series of iterations over the following interlinked steps:
    a. *Reference set selection*: First a reference period is chosen during which the structure is considered to be behaving normally. Measurements collected during this period but without traffic on the bridge are split into training and test sets for the purpose of training regression models and evaluating their performance respectively.

b. *Data preparation*: Measurements are treated for outliers using the interquartile range technique, which has been shown to effectively remove outliers in previous studies [16]. The moving averaging filter is then employed to smooth the measurements to minimize effects of noise. If required, measurements are then down-sampled to an appropriate frequency in order to ensure model training is not too computationally demanding due to the size of the data set. Lastly the dimensionality of the data set of temperature measurements, which will constitute the input to the regression models, is reduced using principal component analysis (PCA), which takes advantage of inherent correlations between variables in the data-set [27]. PCA finds a set of principal component vectors defining an orthogonal transformation from the original set of variables which are linearly-correlated to a new set of variables which are uncorrelated. According to [28], the first one-third of the principal components covers 99.99% of the variability in temperatures. Hence these principal components alone are sufficient as input to the regression models. This step also accounts for thermal inertia effects in the measured data. Thermal inertia refers to the phenomenon of internal material temperatures lagging significantly behind ambient temperatures. Consequently the time series of response and temperature measurements may appear to be out of phase. This is particularly the case in concrete structures due to their voluminous nature, high thermal mass and low thermal conductivity. Thermal inertia effects are effectively incorporated within the regression models by providing the principal components corresponding to temperatures measured at both the current time-step and a previous time-step as input [22,29].

c. *Training and evaluation of regression models*: In this step, regression models are trained using the training data sets. The performance of the trained models is evaluated subsequently on test data sets. The above-mentioned steps are performed iteratively for various kinds of regression models such as support vector regression (SVR) and multiple linear regression. For any chosen regression algorithm, the models are generated iteratively by varying parameter settings until improvements in prediction accuracy are observed to be negligible. However since results from previous studies [22] on thermal response prediction that have compared various types of regression models support the effectiveness of SVR for this task, results using SVR models alone are shown in this paper.

2) Model application phase: In this phase, regression models offering the highest prediction accuracy are employed to predict real-time thermal response from measured temperature distributions. First temperature measurements are prepared for input to the chosen regression model. Measurements are treated for outliers and smoothed, and their dimensionality is reduced using PCA. The first few principal components are provided as input to the regression models to predict thermal response.

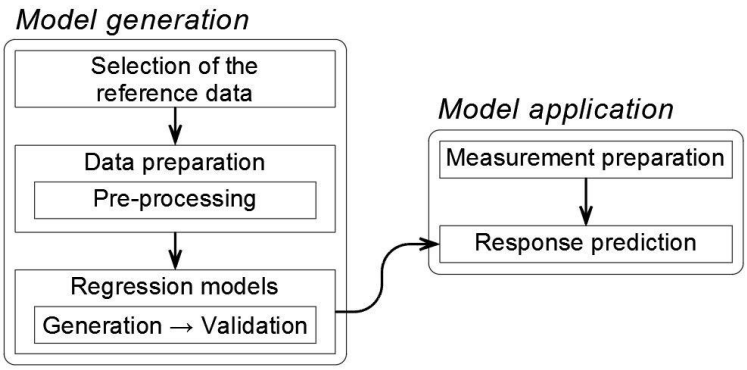

Figure 3 Flowchart showing the strategy for response prediction methodology.

2.2. Traffic-induced response prediction (TIRP) methodology

The TIRP methodology is built on a premise that the traffic-induced response of a bridge can be determined from knowledge of the traffic loads and their locations, and an understanding of the relationship between traffic load parameters and structural response obtained from a set of reference measurements. Theoretically, a single crossing of a vehicle and the respective measured deformations can provide sufficient information to determine relationships between load, its location and response. These relationships can form the basis of regression models that predict displacements induced by similar type of vehicles at any location along the length of the structure. In real-life, however, displacements may not always resemble previously measured values even under the same traffic load. For example, bearings may lock temporarily, creating restraints that change structural behaviour. For these reasons, a broad set of traffic and response data is needed to generate robust and accurate prediction models. Furthermore, temperature effects may persist in the response measurements even after subtracting predicted thermal response using RBTRP methodology as will be shown later in the paper using the case study. This is expected as material properties and hence the structure's stiffness can vary with changes in temperature distributions. For this reason, in addition to information of the magnitude of the applied load and its location, the first few PCs of temperatures are also provided as input variables for the TIRP methodology.

The TIRP methodology follows a process similar to that of the RBTRP methodology (Figure 3) for training and applying regression-based models. Figure 4 illustrates the concept employed to identify the location of a vehicle on a bridge. For the purpose of simplicity, the bridge is assumed to have a single lane and only one vehicle is assumed to be on the bridge at any time. The length of the bridge is split into 100 segments. The segments are numbered sequentially from the left support. The location of a vehicle is defined by the number of the segment in which the centre of the vehicle is located.

In the model generation phase, as for the RBTRP methodology, data set from a reference period is chosen for training purposes. This data set, which includes measurements of temperature distributions and response as well as vehicle loads and locations, is first pre-processed. After removing outliers and noise, thermal response, as predicted by the RBTRP methodology using the temperature measurements, is subtracted from the response measurements to identify the response due to only traffic loads. Using this response data, regression models are trained to

predict the traffic-induced response using the locations and the weights of the vehicles, and the first few principal components of temperature measurements as input. The best models for traffic response prediction are then selected. These models are used in the model application phase (Figure 3) to predict the traffic-induced response in real-time based on measured temperatures and vehicle loads and their locations.

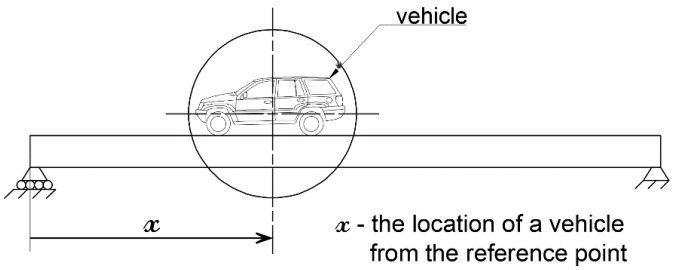

Figure 4 Schematic illustrating input parameters for the TIRP methodology.

After evaluating a number of regression-based techniques for generating models for traffic-induced response prediction, artificial neural networks (ANNs), which are inspired by biological neural systems, have been selected for this study. ANNs are a powerful way of representing nonlinear relationships between a number of input and output parameters [10]. An ANN consists of neurons that are interconnected in various layers. Connections between the neurons have weights that are calibrated during training to capture the actual relationship between the input and output parameters. A key step is the selection of an appropriate architecture of the network that maximizes its efficiency, i.e., use low computational resources while achieving high prediction accuracy [30].

This study uses a multi-layer feed-forward neural network that implements the back-propagation rule [31]. The input parameters to the ANN are locations and weights of moving loads and the first few PC vectors computed from distributed temperature measurements. The output parameters are response values (e.g. strains) at specific locations on the structure. The ANN has one hidden layer and one output layer. The output layer has a single linear neuron. The optimal number of neurons for the hidden layer is found through a trial and error approach that gradually increases the number of neurons while evaluating the performance of the ANN on both training and test sets. A hidden layer of 5 neurons is observed to produce consistently good results. This is in broad agreement with previous research in SHM on the application of ANN for data interpretation that recommend using a hidden layer composed of between 3 and 30 neurons [32,33].

2.3. Anomaly detection techniques

Time histories that result from subtracting the predicted thermal and traffic response from time histories of measured response are analysed for anomalies (damage) using signal processing techniques. The time histories are generated as follows. The differences between measured and predicted response are referred to as prediction errors (PEs), and are computed as shown below:

$$\Delta y_s = p_s - m_s \quad \text{(Eq. 1)}$$

where Δy_s is the PE, and p_s and m_s are predicted and measured response respectively at sensor s. m_s is computed as the sum of the predicted thermal response and the predicted traffic response. The PEs computed for each time-step for a sensor are sequenced chronologically to form a time series, which is referred to as a PE signal.

PE signals are expected to be stationary with a zero mean. Only changes to structural performance due to factors unrelated to loading such as damage are expected to be left in the signals. Such changes in signals are hard or impossible to identify without employing signal-processing techniques. PE signals corresponding to various sensor locations can either be analysed individually or be analysed in groups to detect anomalous structural behaviour. The latter approach, also termed multivariate analysis, relies on the correlations between response measured at various locations of a bridge. Damage to a bridge component will modify prior correlations since bridges are typically well-connected structural systems such that damage affects load paths within the structure. In previous studies, signal subtraction method (SSM) [28] and cointegration [15] have been shown to detect anomaly events better than other signal processing techniques such as moving principal component analysis and moving fast Fourier transform [34]. Therefore, in this study, SSM and cointegration are employed to analyse PE signals for anomalies.

SSM is a novel technique proposed in [28]. In SSM two PE signals are linearly combined to generate a subtracted signal, which is then analysed for anomalies. Mathematically, it is applied as follows:

$$T_{kl} = \left(\frac{w_k}{f_k}\right)\Delta y_k - \left(\frac{w_l}{f_l}\right)\Delta y_l \qquad \text{(Eq. 2)}$$

T_{kl} is the subtracted signal resulting from the subtraction process. Δy_k and Δy_l are values of the PE signals corresponding to sensors k and l respectively. f_k and f_l are scaling factors for the two PE signals. These are equal to the range of signal values in the training period, i.e., the difference between the maximum and minimum values in the training period. w_k and w_l are weights specified according to the accuracies of the respective sensor and its corresponding model for thermal response prediction. In this study, the hypothesis is that measurements from all elements are equally important. Therefore weights of all PE signals are set equal to 1.

Cointegration utilizes the statistical properties of cointegrated signals for anomaly detection. In probability theory, a signal is said to be stationary, if its mean, variance and autocovariance stay constant over time, and non-stationary if otherwise. A non-stationary signal is said to be integrated to an order d if a process of taking differences over the time series repeated d times leads to a stationary signal. In mathematical notation, the order of integration of a signal is often denoted by $I(d)$. A group of signals, where each signal is $I(1)$, is said to be cointegrated if there exists a linear combination of the signals that is stationary. These stationary signals are referred to as cointegrated signals, and the process of finding them referred to as cointegration. The concept of cointegrated signals, which was initially proposed and used in the field of econometrics [35], was first applied to structural health monitoring by Cross et al. [15]. Cross et al. [15] showed that it is useful for purging quasi-static effects in measurements, and

demonstrated its performance using measurements from a few benchmark problems including the National Physical Laboratory Footbridge in the UK [36].

In this paper, cointegration is applied on PE signals, which are typically non-stationary processes since the predicted structural response does not perfectly match the measured response. The premise is that the stationarity of a cointegrated signal derived from PE signals will be affected by an anomaly event. Given n PE signals, $n-1$ cointegrated signals can be generated. Cointegrated signals are generated and evaluated within the MATLAB environment as explained below. The full details of the mathematics behind cointegration can be found in [15].

- Step 1 Test PE signals for stationarity. Non-stationary signals are then converted to signals that are integrated to order one. Augmented Dickey-Fuller [37] test is used to examine the stationarity of a signal. The `adftest` function provided in the MATLAB Econometrics Toolbox [38] is used for this test.
- Step 2 Select signals which have passed the Augmented Dickey-Fuller stationarity test.
- Step 3 Apply the Johansen cointegration procedure [39] to find suitable cointegrating vectors. In this study, the `jcitest` function in MATLAB Econometrics Toolbox [38] is used to find the cointegrating vectors.
- Step 4 Project response measurements into the space of cointegrated vectors. These projected vectors are termed cointegrated residuals and when sequenced chronologically form cointegrated signals.

Both SSM and cointegration fundamentally require computing and tracking the time-evolution of a damage sensitive feature. An anomaly is said to be detected when the evaluated damage sensitive feature, which is a subtracted signal when using SSM and a cointegrated signal when using cointegration, exceeds a predefined confidence interval. Mean (μ) and standard deviation (σ) values during the reference period are computed to derive thresholds for the confidence interval:

$$[\mu - n\sigma, \mu + n\sigma] \quad \text{(Eq. 3)}$$

where n is the number of standard deviations defining the range of the confidence interval. According to previous studies, $n = 3$ and $n = 6$ are chosen to set confidence intervals for damage sensitive features in cointegration and SSM, respectively. Both anomaly detection techniques are briefly described below giving particular attention to the damage sensitive features used in this study.

3. Case study

The performance of the measurement interpretation approach proposed in the previous section is evaluated on measurements collected from a laboratory structure: a truss that is subjected to accelerated temperature variations and periodically applied moving loads.

3.1. Experimental setup

A sketch of the truss depicting its principal dimensions and the location of sensors is shown in Figure 5. Further details on the truss are available in authors' previous work [28]. Temperature variations are simulated with three infrared heating lamps (Figure 5). They are installed 0.5 m above and 0.2 m behind the truss. The lamps are plugged in to the mains through timer plugs which turn them on every 1½ hours for ¾ of an hour. This set-up allows simulating 16 temperature cycles in a day. Temperatures in the truss are monitored with 31 thermocouples and a thermal imaging camera (TIC).

Moving loads are simulated using a mobile platform installed on the bottom chord of the truss (Figure 5) that is driven by a motor. While the speed of the moving platform can be adjusted by altering the power supply to the motor that drives it, the maximum speed at which the platform can be pulled is still much lower than the average speeds of vehicles crossing full-scale bridges. A heating element in the form of a one-watt power resistor is attached to the moving platform. The location of the moving load is detected by processing thermal images, and is defined in terms of its distance from the left support of the truss by assuming that the total length of travel of the platform is 100 units. This concept is shown in Figure 6.

Weights are added onto the platform to simulate traffic loads. This study uses five different moving load cases – 0 N, 40 N, 100 N, 140 N and 180 N, which are from hereon denoted as L-0, L-1, L-2, L-3 and L-4 respectively. Each non-zero load case is applied for up to four simulated diurnal cycles. The weights are altered only when the platform is at the right end of the truss, and the motor is turned off. For case L-0 that is without traffic loading the platform is kept stationary at the right end of the truss. The structure's response is measured at various locations (see Figure 5) with 9 linear-pattern foil strain gauges. Response measurements are collected at a rate of six measurements per minute.

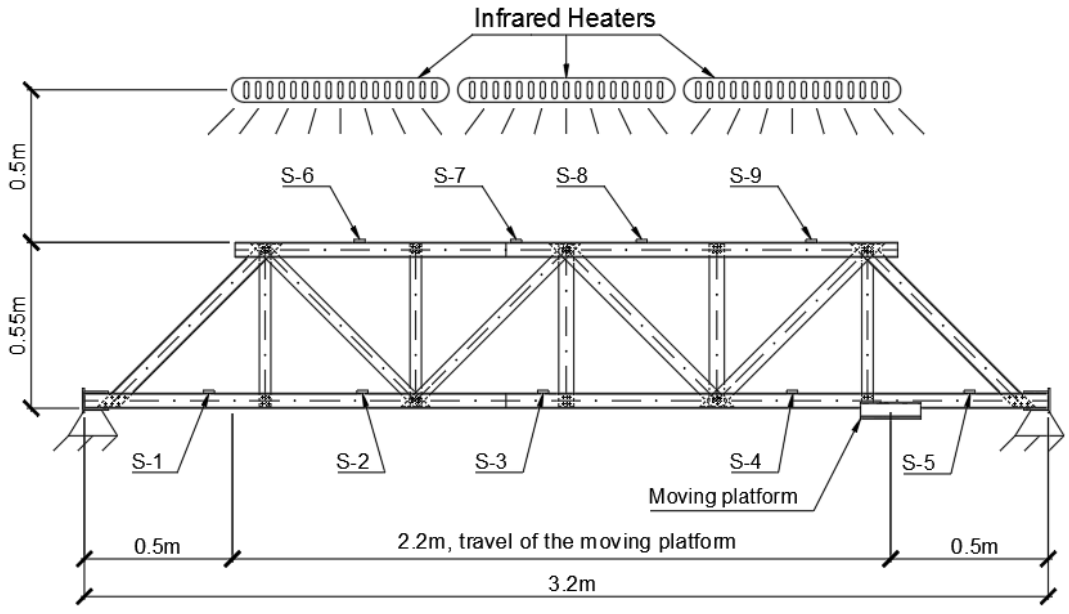

Figure 5 A sketch of the test-bed with its principal dimensions and the location of strain gauges (S-*i, i = 1, 2, ..., 9*).

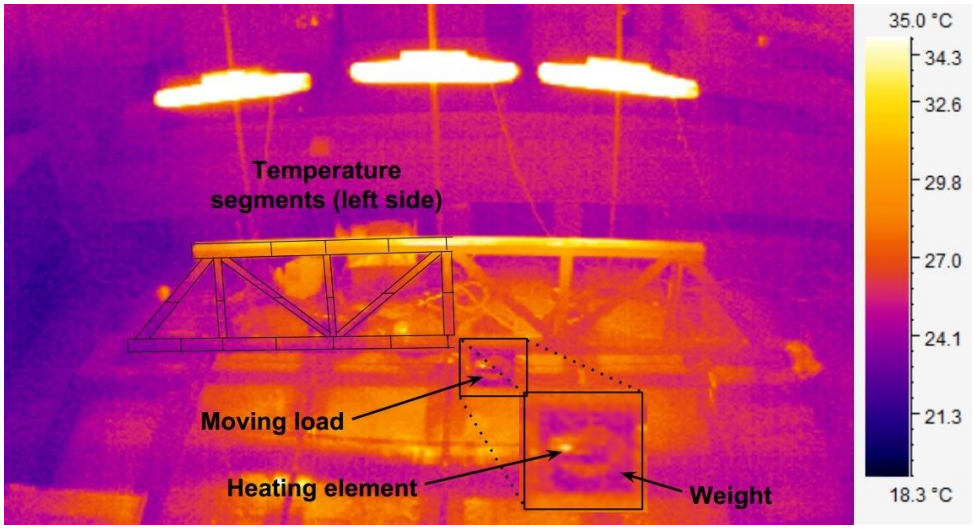

Figure 6 Thermal image of the experimental set-up with a close-up view of the moving load and heating element.

Damage scenarios

The truss is monitored in both healthy and damaged states. Three damage scenarios, which are referred to as DM1, DM2 and DM3, are considered. These scenarios are shown in Figure 7 and listed below:

DM1 - Three bolts are removed from the joint connecting two diagonal and one vertical elements to the bottom chord;
DM2 - Two additional bolts are removed from the same joint named in DM1;
DM3 - Three bolts are removed from a joint on the top chord.

Scenarios DM1, DM2 and DM3 last for 47, 46 and 46 simulated diurnal cycles (or approximately 25,000 measurements in total). At the end of scenario DM3, the truss is repaired by putting back all the removed bolts; this event is denoted as scenario F.

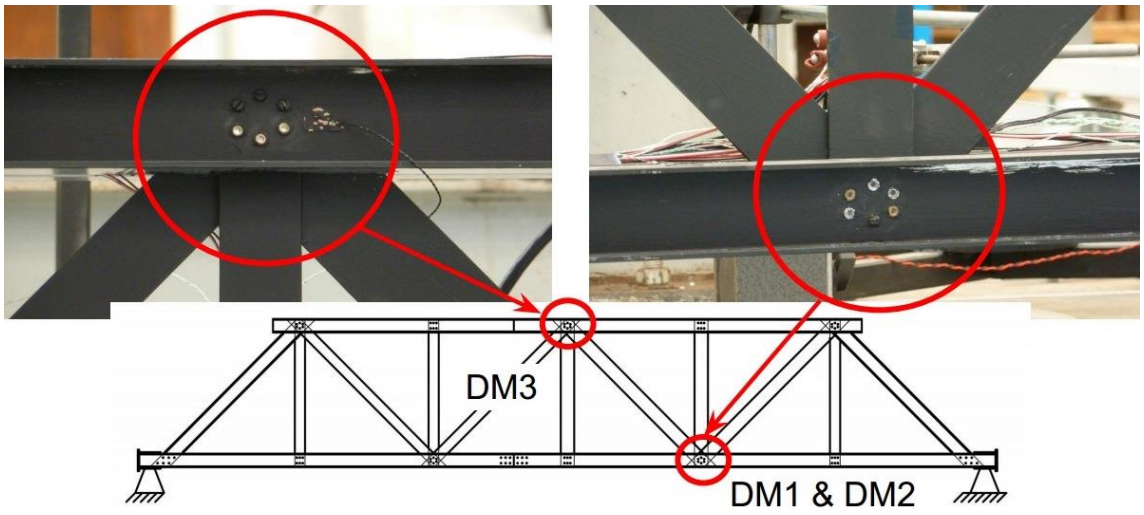

Figure 7 Joints affected by simulated damage scenarios.

3.2. Measurement time histories

Temperatures

Temperature time histories are derived from thermal images collected by the TIC and the measurements from the thermocouples. Thermal images are processed as follows. The area of the truss in the thermal images is divided into segments (see Figure 6). The average temperature is calculated for each segment from each thermal image. In total, 42 segments are created as follows:

- the top and bottom chords are divided in 8 and 12 segments each, and
- each element between the top and bottom chords is split into two segments leading to 22 segments in total.

Temperature variations computed for the top and bottom chords are shown in Figure 8 (left). The plots show that the temperature in the laboratory is affected by the outside air temperature. The temperature variations induced by the infrared heaters are superimposed on the variations in the ambient temperature. A closer look at the time histories reveals the simulated diurnal cycles (Figure 8 (right)). The time histories also show disruptions to data collection, outliers and noise, commonly seen also in measurements from full-scale structures. Disruptions were due to problems related to storing the thermal images. These disruptions are removed to have continuous measurement-histories. Outliers were generated occasionally when the field-of-view of the TIC was partially blocked such as during the presence of a human when the weights on the moving platform are modified.

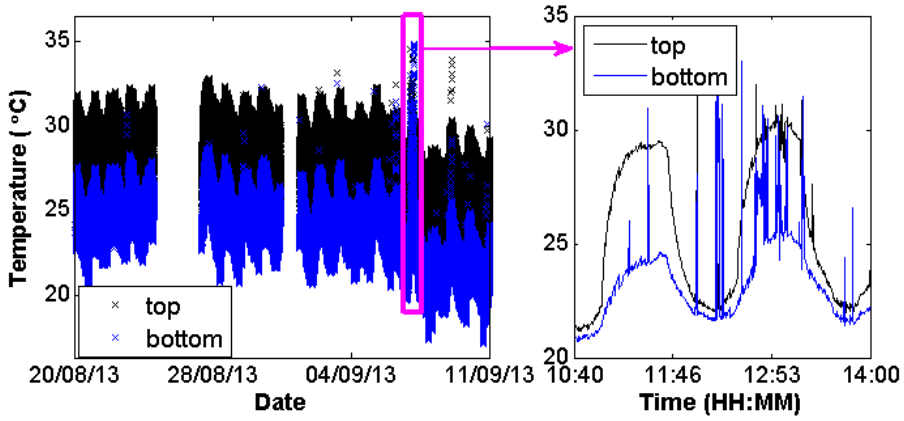

Figure 8 Time histories of temperatures calculated from segments of the top and bottom chord (Figure 6) with those for the entire monitoring period on the left and a closer look at two simulated diurnal cycles on the right.

Response

Response measurements have been collected with no interruptions. However, in order to keep them compatible with the temperature signals, measurements corresponding to periods when thermal images have not been recorded are omitted from response time histories. Figure 9 shows plots of the measurement time histories produced by sensor S-2. The plot on the left shows the first 36,000 measurements in the time histories. The figure also includes closer views of response variations during a simulated diurnal cycle. The plots show that variations in

ambient temperature as well as the radiation from the infra-red lamps affect the structural response.

The response due to the moving loads are seen superimposed on the response due to simulated diurnal cycles in the form of a noisy pattern (Figure 9 (middle)). Strains spike when the moving platform passes by the sensor location S-2 (see Figure 9 (right), between measurements #100 and #150). The complete strain signals produced by sensors S-4, which are located close to the joint involved in damage scenarios DM1 and DM2, are shown in Figure 10. Strain measurements closely resemble variations in temperatures (Figure 10). While a gradual drift of the signal is observed after damage event DM2, at this time the ambient temperature has also decayed (see Figure 8 around 7/11/2013).

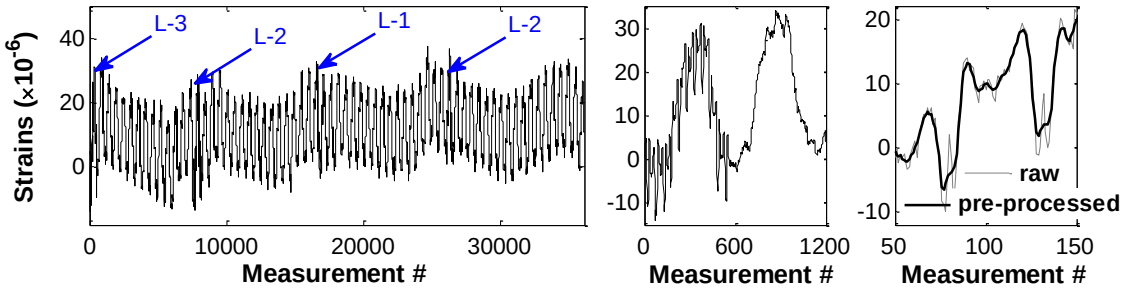

Figure 9 Strains measured with sensor S-2 (right) and closer views (middle and left) of the time histories to understand the effects of moving load.

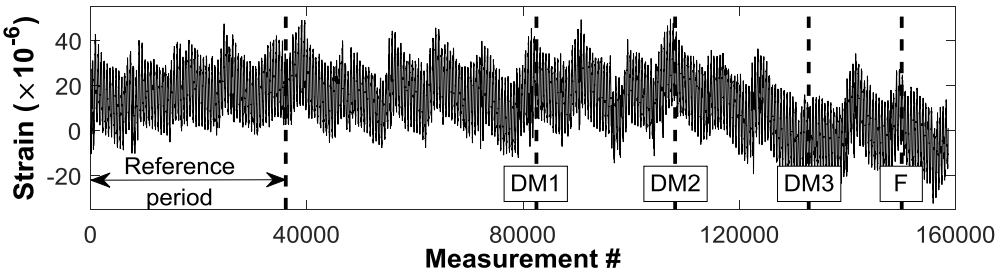

Figure 10 Strain signals as measured with S-4; also shown are the time of initiation of the various damage scenarios.

Figure 11 shows strain signals in relation to the location of the moving load as computed from the thermal images. The correlations between the strains and locations of the moving load are such that the location of the moving load can even be defined accurately from the measured response.

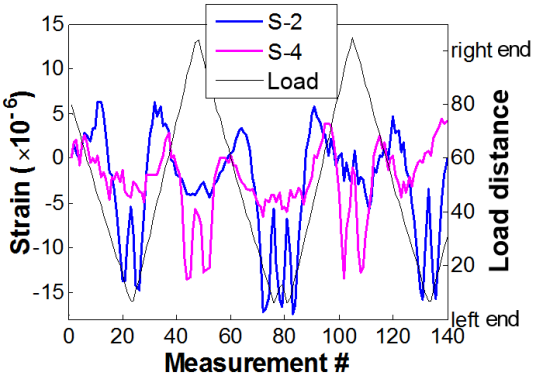

Figure 11 Locations of the moving load computed from thermal images plotted alongside strains.

4. Results

In this section, the proposed measurement interpretation approach is evaluated on measurements collected from the laboratory truss. The RBTRP methodology and then the TIRP methodology are employed to generate statistical models for predicting temperature-induced and traffic-induced response respectively. The PE signals, which are derived after purging the effects of temperature and traffic loads from measurement time histories, are then processed using anomaly detection techniques.

4.1. Response predictions

Reference period

Measurements from the first 66 simulated diurnal cycles (see Figure 10) form the reference period for evaluating the proposed approach. Measurements taken during this period are plotted in Figure 9 (left). Periods when the moving load is present, are excluded from the reference data-set for the RBTRP methodology. The four periods when the moving load is present in the reference period as indicated in Figure 9 (left) form the reference-data set for the TIRP methodology. Load L-4 has not been deployed during the reference period. This study will examine if the response due to L-4 can be predicted accurately using regression models that are generated based solely on the loads present during the reference period.

Thermal response prediction

The RBTRP methodology is employed to derive regression models to predict thermal response. Regression models are generated using temperatures collected using the TIC. High prediction accuracies, as evaluated in terms of root mean square error (RMSE), are obtained for strain predictions when:

- the input temperature measurements are down-sampled to 1.2×10^{-2} Hz,
- the number of PCs is set to 14, and
- the PCs corresponding to the current time-step and the previous time-step are provided as input to the regression models for accounting for thermal inertia effects.

A PE signal computed for sensor location S-2 is plotted in Figure 12. A PE signal for a specific sensor is denoted as PE *sensor name*, for example, PE S-2 refers to a PE signal for sensor location S-2. If noise in thermal response predictions and measurement noise follow a Gaussian distribution, the PE signals will resemble a stationary signal. A deviation from stationarity such as in the form of a change to the mean of the signal may indicate the presence of the moving load. Spikes due to the moving loads are discernible in PE S-2 shown in Figure 12. A closer examination of PE S-2 during the period when load L-2 is applied reveals that thermal effects have not been fully removed from response measurements (Figure 12 (right)). PE values at the sensor location S-2 rise abruptly from 0 to 15×10^{-6} when the moving load is applied (near measurement #7510). With respect to damage scenarios, a gradual shift in the mean of PE S-2 can be noticed shortly after scenario DM2. However, other scenarios are not detectable from the PE signals.

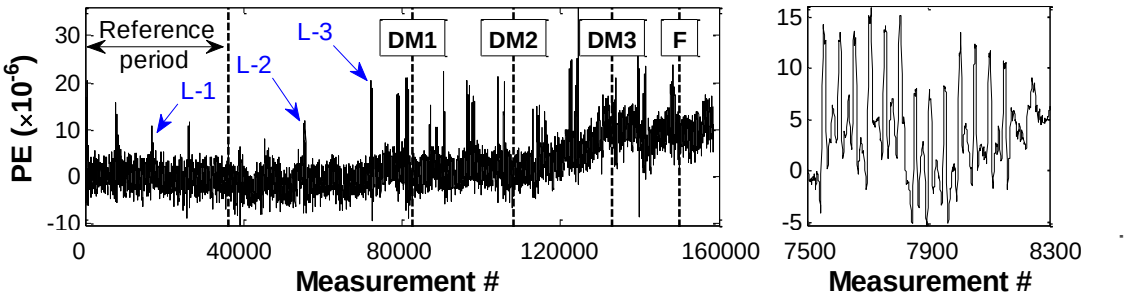

Figure 12 The variation of PEs for sensor location S-2 is plotted to show the effect of the moving load and temperature (left), and a closer view of the signal (right).

Next, regression models are generated using temperature measurements from thermocouples in order to compare its performance with those generated using measurements from the TIC. As when using data from the TIC, temperature measurements are down-sampled to 1.2×10^{-2} Hz. 10 PCs are required to capture 99.99% of the variability in temperature measurements.

Table 1 presents data on the accuracy of the regression models produced for thermal response prediction using temperature data from thermocouples and the TIC. The accuracy is expressed using a parameter e_p, which is a measure of error computed in terms of the range of measured strains for a group of sensors (see Eq. 4).

$$e_p = \frac{1}{n}\sum_{s=1}^{n}\frac{e_s}{r_s} \quad \text{(Eq. 4)}$$

n is the number of sensors; e_s is the root mean squared error in predictions and r_s is the range of measured strains at sensor s. The sensors on the top and bottom chords are analysed separately in two groups. The mean range of the measured strains is:

- 68×10^{-6} strains collected with five strain sensors on the bottom chord;
- 138×10^{-6} strains collected with four strain sensors on the top chords;

Results in Table 1 show that regression models generated using temperature measurements collected by both TIC and thermocouples demonstrate high accuracy.

Table 1: Accuracy (expressed in terms of e_p) of the regression models generated using temperature measurements from thermocouples (noted as TH in the table) and the TIC.

	Bottom chord (strains)		Top chord (strains)	
	TH	TIC	TH	TIC
e_p (%)	4.2%	3.7%	1.8%	1.8%

Traffic-induced response predictions

The PE signals computed using measurements from the TIC are next treated for effects of the moving loads. The results presented in Figure 12 (right) show that temperature effects are still present even after subtracting predicted thermal response from the measured response. This is evident from the underlying sinusoidal variation in the trend, which corresponds directly to the simulated diurnal cycle. For this reason, predicting the vehicular response requires information regarding temperatures. Hence information of the magnitude of the applied load and its location and the first few PCs of temperatures are selected as input variables for the TIRP methodology. Combinations of the measurement input frequency and number of PCs are evaluated. The best results are found when the input traffic measurements are down-sampled to 5×10^{-2} Hz and the number of PCs is set to 4.

The predicted and measured traffic-induced response for three periods over the monitored duration are provided in Figure 13. These periods are described below:

- Period A, which is within the reference period, and comprises measurements #7,000 to #8,100 during which load L-2 is applied (Figure 13 (left));
- Period B, which is outside the reference period but before the introduction of damage scenarios, and comprises measurements #55,200 to #55,600 during which load L-2 is applied (Figure 13 (middle)), and
- Period C, which is outside the reference period but before the introduction of damage scenarios, and comprises measurements #81,100 to #81,500 during which load L-4, a moving load unexperienced during the reference period, is applied (Figure 13 (right)).

Predicted and measured strains are in good agreement for periods A and B. However, the discrepancy in predictions is comparatively large for the period C (Figure 13 (top)) when L-4 was applied. Response due to L-4 cannot be predicted accurately using regression models that are generated based solely on the loads present during the reference period. Hence, all types of loads have to be included in the regression model generation. A plot of PE S-2 is provided in Figure 14.

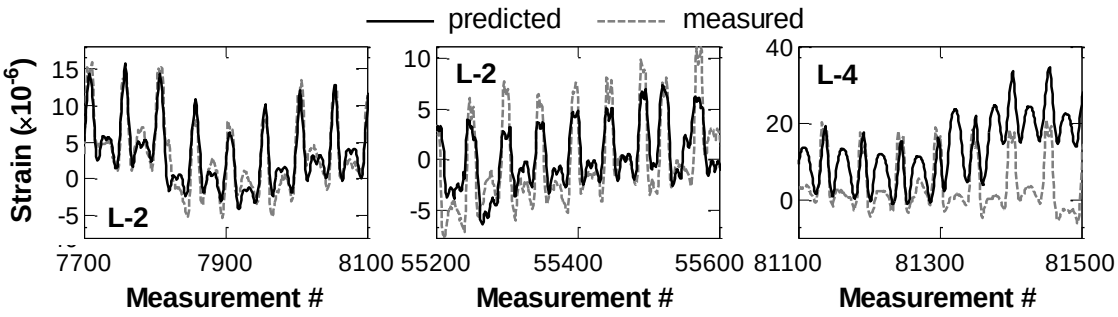

548

549

550 Figure 13 Measured and predicted strains during period A (left), period B (middle) and
551 period C (right).

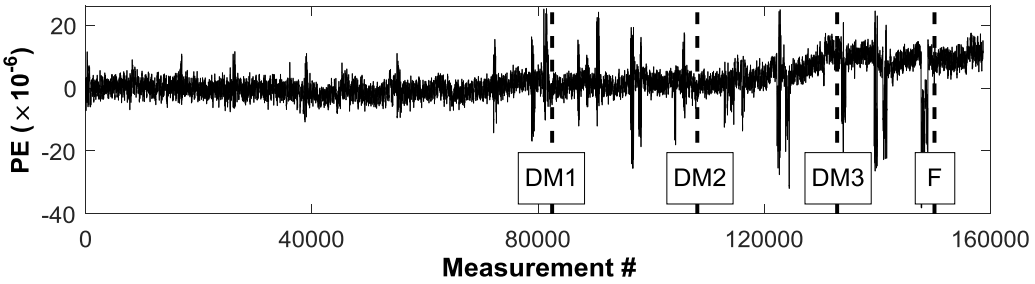

552

553 Figure 14 PE signals derived after subtracting traffic-induced and thermal response from
554 measurements collected by sensor S-2.

555 ## 4.2. Anomaly detection

556 In this section, anomaly detection techniques are employed to interpret the time histories of
557 data. First, anomaly detection techniques are used on prediction error signals computed by
558 subtracting both predicted thermal and traffic response from measured response. Next, to
559 understand the effectiveness of subtracting traffic response from the measurements, anomaly
560 detection techniques are used on the error signals computed by subtracting only predicted
561 thermal response from measured response. Then, anomaly detection techniques are employed
562 directly on the time histories of response measurements to demonstrate the importance of
563 having models to predict thermal and traffic-induced response.

564 **Interpretation of prediction error (PE) signals**

565 Cointegration: The PE signals derived in Section 4.1 are first analysed for anomaly events with
566 the cointegration technique. The first ⅓rd of measurements from the reference period forms the
567 data-set used to derive the cointegration model. The confidence interval is defined using values
568 of cointegrated residuals from the reference period. The computed cointegrated signal is plotted
569 in Figure 15. Spikes and temporary shifts in the signal are indicative of periods when moving
570 loads are present. The larger spikes before DM1 represent periods when L-4 is applied. Values
571 of cointegrated residuals are observed to deviate away from the confidence interval as the
572 damage severity increases. The trend departs gradually from the confidence interval after DM1
573 and it permanently departs the confidence interval after DM2.

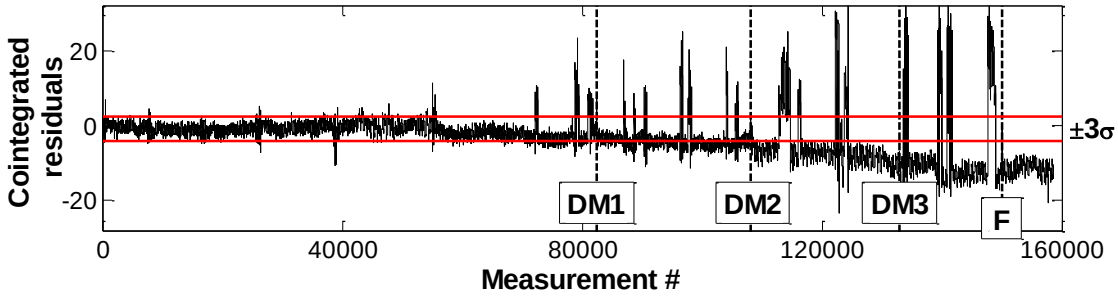

Figure 15 Cointegrated residuals of signals computed in Section 4.2.

SSM: Two PE signals are combined to create one SSM signal. For example, subtracted signal T_{S1S5} is a combination of PE signals from sensor location S-1 and S-2. For DM1 and DM2, the joint that lies between sensor locations S-3 and S-4 is damaged. The subtracted signals created from the signals corresponding to the two sensor locations are expected to reflect anomaly events. However, all combinations of PE signals from strain sensors located on the bottom chord show evidence of anomaly events, and especially subtracted signals created from those signals corresponding to sensors S-1 and S-2. Figure 16 plots three subtracted signals – T_{S1S5}, T_{S2S4} and T_{S2S5}, all of which indicate anomaly events. Similar to cointegrated signals, periods when the moving loads are present can be seen as spikes in values of subtracted residuals. T_{S1S5} and T_{S2S5} permanently exceed the confidence interval after DM2. T_{S2S4} departs from the confidence interval soon after DM1. T_{S2S4} deviates further from the upper bound of the confidence interval with increasing damage severity. When the structure is mended at event F, the signal tends to return to the confidence interval. The values of subtracted residuals of other signals hold steady after the truss is repaired during event F.

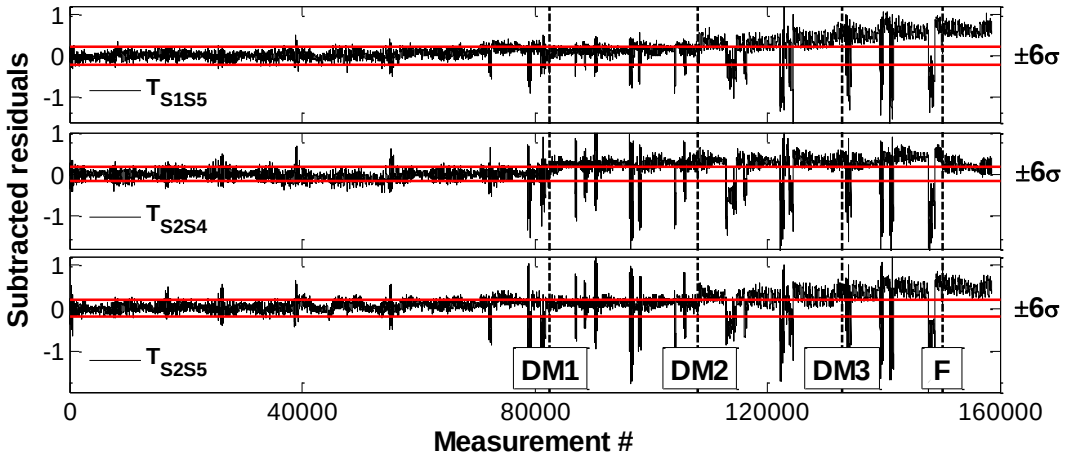

Figure 16 SSM residuals T_{S1S5}, T_{S2S4} and T_{S2S5} for signals computed in Section 4.1.

Interpretation of signals without thermal response

In order to assess the impact of moving loads on anomaly detection, measurements taken without having moving loads on the structure are now analysed separately. PE signals derived from subtraction of the thermal response from these measurements are analysed using anomaly detection techniques. When the periods of moving loads are excluded from the measurement interpretation, signal trends become much less noisy. As an example, a cointegrated signal is

generated and plotted in Figure 17. The cointegrated signal has a few spikes and has no shifts when compared to the cointegrated signal plotted in Figure 15. Shifts in the signal due to anomaly events are distinguishable, especially those due to anomaly events DM1, DM3 and F. Similar results are achieved when interpreting the same data-set with SSM. They are not plotted here for reasons of brevity.

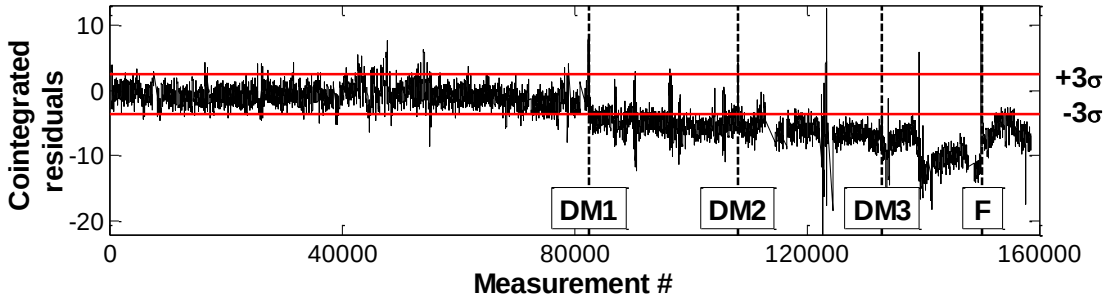

Figure 17 Cointegrated residuals generated from PE signals for measurement periods when no moving load is present.

Interpretation of response measurements

A plot of a cointegrated signal generated using collected strain measurements is provided in Figure 18. The signal starts to drift gradually from the confidence interval shortly after DM2, and the signal permanently departs the confidence interval after DM3. Figure 15 and Figure 17 show that anomaly events can be detected sooner by analysing the signals generated after subtracting traffic-induced and thermal response than by direct analysis of response measurements. This conclusion of faster and more reliable damage detection using PE signals has already been confirmed [34].

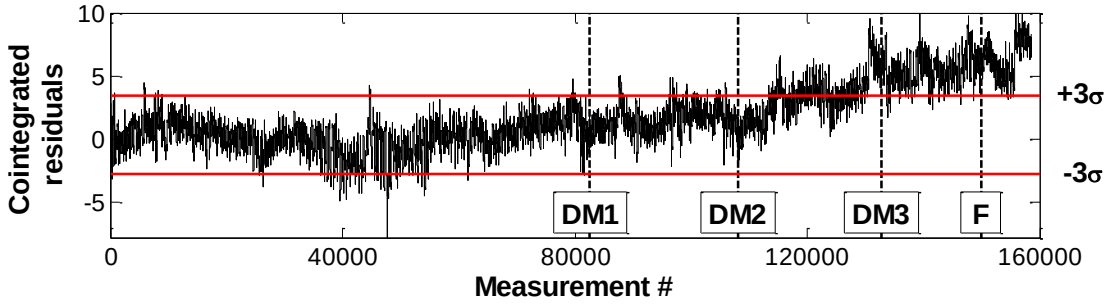

Figure 18 Cointegrated residuals of strain measurements.

4.3. Application of the temperature-based measurement interpretation approach

This study lastly evaluates the application of the temperature-based measurement interpretation approach proposed in [28]. The idea here is to evaluate if thermal effects alone can form the basis of measurement interpretation without giving consideration to the presence or absence of moving loads on the structure. Comparing results from this approach with those presented in Sections 4.1 and 4.2 using TIRP methodology will enable us to ascertain if knowledge of traffic loads helps with measurement interpretation.

The temperature-based measurement interpretation approach is similar to the measurement interpretation approach presented in Section 2 but with two key differences. First, it does not include the TIRP methodology. Second, training of the regression models in RBTRP methodology is done using all available data during the reference period including response data collected when moving loads are present.

Response predictions: The reference period used for the regression model generation of thermal response prediction is the same as used in Section 4.1, i.e. 66 simulated diurnal cycles. However the measurement time histories are not separated into two data sets according to whether they have moving loads or not as described in Section 2. A data-set that comprises all strain measurements including those that have effects of moving loads during the reference period is selected as input to the RBTRP methodology. The e_p (see Eq. 4) values for predictions is 3.2%. These are similar to the error values obtained when the RBTRP methodology is coupled with the TIRP methodology (see Table 1). PE S-2 is plotted in Figure 19, which is similar to the signal shown in Figure 12PE values spike for periods when moving loads are present.

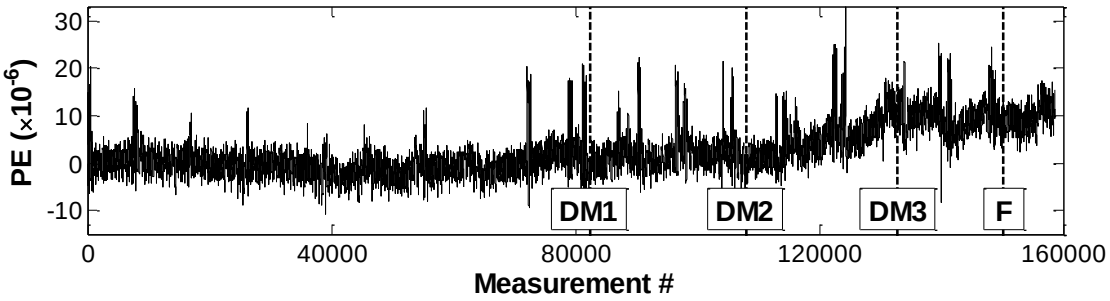

Figure 19 PE S-2 derived from unfiltered strain measurements.

Anomaly detection: PE signals are inspected for anomaly events using the same parameter settings as used in Section 4.2. Both SSM and cointegration show reasonably good and comparable results. For reasons of brevity, signals generated using SSM only are discussed. T_{S1S5}, T_{S2S4} and T_{S2S5} (similar to those shown in Figure 16) are plotted in Figure 20. Drifts in subtracted signals are not as emphasized as in the signals plotted in Figure 16similar. The onset of damage can be recognized only in T_{S1S5} (Figure 20when the signal permanently departs the confidence interval. The other signals are weak indicators of anomaly events.. The other signals are weak indicators of anomaly events.

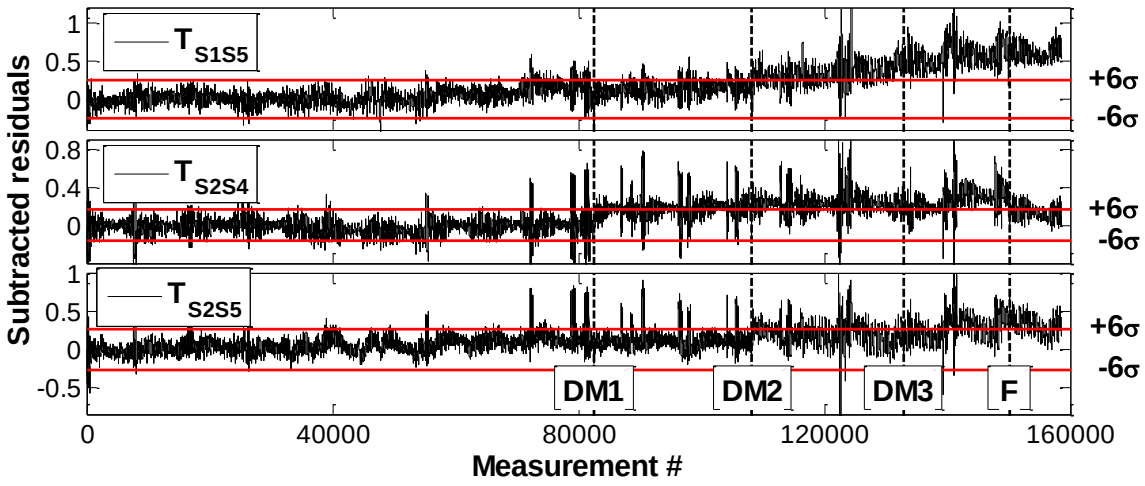

Figure 20 T_{S1S5}, T_{S2S4} and T_{S2S5} generated using SSM from PE signals (see Section 0)

4.4. Discussion

This study demonstrates a new contact-free approach of measuring temperatures using a thermal imaging camera (TIC) in the context of continuous bridge monitoring. Results show that thermal response can be predicted accurately from the temperature distributions measured by either a TIC or thermocouples (see Figure 6 and Figure 8). These results are validation of the performance of the RBTRP methodology, also demonstrated previously by the authors in [22].

The selection of reference period is observed to be a key factor in the performance of the TIRP methodology. The regression models failed to predict the traffic response for load case L-4 when measurements corresponding to this loading scenario were not included in the training data set (see Figure 13). In real-life, this would imply that the regression models would not perform suitably for abnormal loading scenarios, which may be absent or appear rarely in the reference data set. However, for loading scenarios that are present in the training set, the regression models predict the traffic response with sufficient accuracy.

Results from the application of anomaly detection techniques on prediction error (PE) signals and other signals computed without removing the traffic response offer interesting insights. Both SSM and cointegration are capable of detecting some anomaly events from PE signals. Cointegrated signals and subtracted signals show shifts after damage scenario DM-1 but these are not significant enough (i.e. do not exceed threshold bounds) to confirm an anomaly event. However, incremental damage through DM-2 does eventually take the signals outside the threshold bounds (Figure 15 and Figure 16). If the threshold bounds were calibrated after DM-2, the cointegrated signal may have also detected DM-3. None of the signals return to their original position after scenario F when the truss is repaired. This may indicate that the connection stiffnesses of the joints, where bolts were removed, were permanently altered and were not taken back to their original states when the same bolts were re-inserted. The anomaly detection techniques perform better when applied on the portion of the measurements that are without traffic response (see Figure 17). This indicates that, on bridges where there are periods with minimal vehicle loading, the proposed approach can be adapted to analyse measurements

that contain only thermal response. A lot of short- and medium-span bridges in the road network have significantly less traffic during night times and may fall in this category.

Anomaly detection techniques show better performance when applied on PE signals than when applied directly on response time series. This indicates that subtracting thermal response and vehicle response from response measurements improves the chances of anomaly detection. The particular importance of subtracting vehicle response is confirmed by the last set of results on the performance of the temperature-based measurement interpretation approach that ignores the presence or absence of traffic loads while accounting for thermal response. These results support the idea of devising measurement interpretation techniques that focus on explicitly accounting for the effect of various loads (e.g. traffic, temporary works) and environmental parameters (e.g. temperature, wind) to support reliable detection of anomaly events. Lastly, it must be noted that anomaly detection techniques are meant to support engineers in decision-making. Engineering judgment and knowledge will be required to decide on the course of action upon notification of an anomaly event. Actions could be in the form of on-site inspections and augmentation of the monitoring system.

4.5. Limitations

The focus of this study is on the interpretation of measurements rather than measurement collection, which can itself be a challenging task. For instance, most highway bridges have continuous traffic flow on multiple lanes and will require sophisticated vision-based monitoring systems to capture data on the traffic and its loads. The collection of images and their subsequent processing to produce data on the locations and weights of the vehicles is a computational challenge that is solvable [40].

The case study used in this study is a laboratory setup of a much smaller scale than a real-life structure. In a full-scale bridge, strain measurements have dynamic effects that are determined by the weight and the speed of the vehicle and the profile of the road surface in addition to the bridge structural characteristics (e.g. natural frequency). Also, only one vehicle was considered to be on the laboratory structure at any given time, an aspect which is not true in real-life bridges. A natural next step is therefore to test and evaluate the proposed approach using measurements from potentially a short-span full-scale bridge.

5. Conclusions

A novel measurement interpretation approach to predict traffic-induced and thermal response of bridges using measurements of distributed temperature and traffic loads and their locations is proposed in this paper. This approach is investigated using measurements from a laboratory structure that is exposed to accelerated temperature variations. Traffic loads are simulated using a moving platform that travels along the bottom chord of the truss and can hold adjustable weights. Response measurements are collected with contact sensors (e.g. strain gauges), and temperature distributions are captured with a thermal imaging camera and thermocouples. The structure is monitored in health and damaged states. Traffic-induced and thermal response are predicted and subsequently removed from the measured response time histories. In the process,

718 prediction error signals are created. These signals are then interpreted with anomaly detection
719 techniques.

720 This experimental study draws the following conclusions:

721 • Thermal images can be used to measure temperature distributions at accuracies
722 sufficient for data interpretation. Both regression models generated with temperature
723 measurements from the thermal imaging camera and from the thermocouples show high
724 prediction accuracies.
725 • When moving loads are present, thermal effects are not removed completely from
726 response measurements by predicted thermal response. For this reason, in addition to
727 information of the magnitude of the applied load and its location, the first few PCs of
728 temperatures are also needed as input variables for the TIRP methodology.
729 • All types of traffic loads have to be included in the reference period to create robust
730 statistical models for traffic-induced response prediction. If certain load cases are
731 excluded, then TIRP fails to accurately predict traffic response for those scenarios.
732 • The proposed TIRP methodology is unable to fully eliminate the effect of moving loads
733 on measured response. Consequently anomaly detection is observed to be better when
734 measurements collected during traffic loads are excluded from the data set.

735 The proposed integrated approach needs further development to integrate a broader range of
736 traffic scenarios and validation on measurements from real-life structures with high thermal
737 mass. The TIRP methodology, which aims to predict traffic-induced response, needs further
738 integration with sensing technologies for applications to full-scale structures. TICs need to be
739 employed continuously on full-scale bridges to certify their scalability. In the experimental
740 setup, the laboratory truss was coated with a matt black paint hence reduction surface reflection
741 which might be an issue when monitoring full-scale bridges.

742 # 6. References

743 [1] J. Brownjohn, Structural health monitoring of civil infrastructure, Philos Trans. A Math
744 Phys Eng Sci. 365 (2007) 589–622.

745 [2] R.S. Adhikari, O. Moselhi, A. Bagchi, Image-based retrieval of concrete crack
746 properties for bridge inspection, Autom. Constr. 39 (2014) 180–194.
747 doi:10.1016/j.autcon.2013.06.011.

748 [3] Roads Liaison Group, Management of Highway Structures - A Code of Practice, 2013.

749 [4] UK Transport Committee, Memorandum from UK Roads Liaison Group, 2010.
750 http://www.publications.parliament.uk/pa/cm200910/cmselect/cmtran/473/473we04.ht
751 m.

752 [5] FHWA, Tables of Frequently Requested NBI Information, (2015).
753 https://www.fhwa.dot.gov/bridge/britab.cfm (accessed August 30, 2016).

754 [6] E.J. Cross, K.Y. Koo, J.M.W. Brownjohn, K. Worden, Long-term monitoring and data
755 analysis of the Tamar Bridge, Mech. Syst. Signal Process. 35 (2013) 16–34.
756 doi:http://dx.doi.org/10.1016/j.ymssp.2012.08.026.

757 [7] H. Sousa, C. Félix, J. Bento, J. Figueiras, Design and implementation of a monitoring

system applied to a long-span prestressed concrete bridge, Struct. Concr. 12 (2011) 82–93.

[8] R. Kromanis, P. Kripakaran, B. Harvey, Long-term structural health monitoring of the Cleddau bridge: evaluation of quasi-static temperature effects on bearing movements, Struct. Infrastruct. Eng. 2479 (2015) 1–14. doi:10.1080/15732479.2015.1117113.

[9] D. Inaudi, B. Glisic, Continuous monitoring of concrete bridges during construction and service as a tool for data-driven bridge health monitoring, in: Adv. Bridg. Maintenance, Saf. Manag. Life-Cycle Performance, Proc. Third Int. Conf. Bridg. Maintenance, Saf. Manag., 2006: pp. 421–422. http://www.scopus.com/inward/record.url?eid=2-s2.0-56749155028&partnerID=40&md5=64976977b5ee0174d52531ca750d06e1.

[10] H. Sohn, K. Worden, C. Farrar, Statistical Damage Classification under Changing Environmental and Operational Conditions, J. Intell. Mater. Syst. Struct. 13 (2002).

[11] F.N. Catbas, M. Susoy, D.M. Frangopol, Structural health monitoring and reliability estimation: Long span truss bridge application with environmental monitoring data, Eng. Struct. 30 (2008) 2347–2359.

[12] N. Hoult, P. Fidler, Long-term wireless structural health monitoring of the Ferriby Road Bridge, J. Bridg. Eng. 15 (2010) 153–159. http://ascelibrary.org/doi/abs/10.1061/(ASCE)BE.1943-5592.0000049 (accessed April 5, 2014).

[13] B. Peeters, G. De Roeck, One-year monitoring of the Z 24-Bridge: environmental effects versus damage events, Earthq. Eng. Struct. Dyn. 30 (2001) 149–171.

[14] K. Worden, C.R. Farrar, G. Manson, G. Park, The fundamental axioms of structural health monitoring, Proc. R. Soc. A Math. Phys. Eng. Sci. 463 (2007) 1639–1664.

[15] E.J. Cross, K. Worden, Q. Chen, Cointegration: a novel approach for the removal of environmental trends in structural health monitoring data, Proc. R. Soc. A Math. Phys. Eng. Sci. 467 (2011) 2712–2732. doi:10.1098/rspa.2011.0023.

[16] D. Posenato, P. Kripakaran, D. Inaudi, I.F.C. Smith, Methodologies for model-free data interpretation of civil engineering structures, Comput. Struct. 88 (2010) 467–482.

[17] Y.-L. Ding, G.-X. Wang, P. Sun, L.-Y. Wu, Q. Yue, Long-Term Structural Health Monitoring System for a High-Speed Railway Bridge Structure, Sci. World J. 2015 (2015) 1–17. doi:10.1155/2015/250562.

[18] E. Figueiredo, E. Cross, Linear approaches to modeling nonlinearities in long-term monitoring of bridges, J. Civ. Struct. Heal. Monit. 3 (2013) 187–194. doi:10.1007/s13349-013-0038-3.

[19] R. Kromanis, P. Kripakaran, Support vector regression for anomaly detection from measurement histories, Adv. Eng. Informatics. 27 (2013) 486–495.

[20] I. Laory, T.N. Trinh, I.F.C. Smith, Evaluating two model-free data interpretation methods for measurements that are influenced by temperature, Adv. Eng. Informatics. 25 (2011) 495–506.

[21] I. Laory, T.N. Trinh, D. Posenato, I.F.C. Smith, Combined Model-Free Data-Interpretation Methodologies for Damage Detection during Continuous Monitoring of Structures, J. Comput. Civ. Eng. 27 (2013) 657–666. doi:10.1061/(ASCE)CP.1943-5487.0000289.

[22] R. Kromanis, P. Kripakaran, Predicting thermal response of bridges using regression models derived from measurement histories, Comput. Struct. 136 (2014) 64–77.

[23] M.T. Yarnold, F.L. Moon, A.E. Aktan, Temperature-Based Structural Identification of Long-Span Bridges, J. Struct. Eng. (2015) 1–10. doi:10.1061/(ASCE)ST.1943-541X.0001270.

[24] B. Glisic, M.T. Yarnold, F.L. Moon, A.E. Aktan, Advanced Visualization and Accessibility to Heterogeneous Monitoring Data, Comput. Civ. Infrastruct. Eng. 29 (2014) 382–398. doi:10.1111/mice.12060.

[25] R. Zaurin, F. Necati Catbas, Structural health monitoring using video stream, influence lines, and statistical analysis, Struct. Heal. Monit. 10 (2010) 309–332. doi:10.1177/1475921710373290.

[26] L.E.Y. Mimbela, L.A. Klein, Summary of vehicle detection and surveillance technologies used in intelligent transportation systems, 2000.

[27] I.T. Jolliffe, Principal Component Analysis, Springer-Verlag New York Inc., 2002.

[28] R. Kromanis, P. Kripakaran, SHM of Bridges: Characterising Thermal Response and Detecting Anomaly Events Using a Temperature-Based Measurement Interpretation Approach, J. Civ. Struct. Heal. Monit. 6 (2016) 237–254. doi:10.1007/s13349-016-0161-z.

[29] X.G. Hua, Y.Q. Ni, J.M. Ko, K.Y. Wong, Modeling of Temperature–Frequency Correlation Using Combined Principal Component Analysis and Support Vector Regression Technique, J. Comput. Civ. Eng. 21 (2007) 122–135.

[30] U. Dackermann, Vibration-based damage identification methods for civil engineering structures using artificial neural networks, University of Technology Sydney, 2010.

[31] M. Riedmiller, A Direct Adaptive Method for Faster Backpropagation Learning : The RPROP Algorithm, in: Neural Networks, 1993., IEEE Int. Conf., IEEE, 1993: pp. 586–591.

[32] J. Mata, Interpretation of concrete dam behaviour with artificial neural network and multiple linear regression models, Eng. Struct. 33 (2011) 903–910.

[33] C.E. Katsikeros, G.N. Labeas, Development and validation of a strain-based Structural Health Monitoring system, Mech. Syst. Signal Process. 23 (2009) 372–383.

[34] R. Kromanis, Structural Performance Evaluation of Bridges : Characterizing and Integrating Thermal Response, University of Exeter, 2015.

[35] J.H. Stock, M.W. Watson, Testing for common trends, J. Am. Stat. Assoc. 83 (1988) 1097–1107.

[36] K. Worden, E. Cross, E. Barton, Damage detection on the NPL Footbridge under changing environmental conditions, in: 6th Eur. Work. Struct. Heal. Monit., Dresde, Germany, 2012: pp. 1–8.

[37] D.A. Dickey, W.A. Fuller, Distribution of the Estimators for Autoregressive Time Series With a Unit Root, J. Am. Stat. Assoc. 74 (1979) 427–431. doi:10.2307/2286348.

[38] MATLAB, Statistics Toolbox Release 2016b, (2016).

[39] S. Johansen, Statistical analysis of cointegration vectors, J. Econ. Dyn. Control. 12 (1988) 231–254.

[40] R. Zaurin, F.N. Catbas, Integration of computer imaging and sensor data for structural health monitoring of bridges, Smart Mater. Struct. 19 (2010) 15019. doi:10.1088/0964-1726/19/1/015019.